

Synthesis and Characterization of Water-Soluble, All-Inorganic Composition, Dawson-Type Trisubstituted Heteropolytungstates. Effect of Alkali Metal Counteranions (Li, Na, K, and Cs) on the $P_2W_{15}Nb_3O_{62}^{9-}$ Polyoxoanion

Kenji Nomiya,* Chika Nozaki, Kohji Miyazawa, Yasushi Shimizu, Toshio Takayama,[†] and Keiichi Nomura

Department of Materials Science, Faculty of Science, Kanagawa University, Tsuchiya, Hiratsuka, Kanagawa 259-12

[†]Department of Applied Chemistry, Faculty of Engineering, Kanagawa University, Rokkakubashi, Yokohama, Kanagawa 221

(Received January 6, 1997)

The water-soluble form of the Dawson-type trisubstituted tungstoheteropolyanion, B- α - $P_2W_{15}Nb_3O_{62}^{9-}$, was synthesized as its nona alkali-metal salts of Li, K, and Cs. Analytically pure compounds, obtained as homogeneous colorless solids, had nonahydrate for the nonalithium (Li₉) salt, tetrahydrate for the nonasodium (Na₉) salt, trihydrate for the nonapotassium (K₉) salt and trihydrate for the nonacaesium (Cs₉) salt, respectively, after each was dried overnight at room temperature under 10^{-3} — 10^{-4} Torr. TG/DTA analyses show that they can be made with 25 water for the Li₉ salt, 23 water for the Na₉ salt, 9 water for the K₉ salt, and 8 water for the Cs₉ salt under atmospheric conditions. A compositional characterization was accomplished by complete elemental analyses and TG/DTA, and structural characterization was achieved by a combination of FT-IR and variable-temperature solid-state ^{31}P NMR and by both ^{31}P and ^{183}W NMR measurements at room temperature in D₂O and DMSO-*d*₆ solutions. The amount of hydrated waters, solubility in solvents and ease of crystallization were significantly influenced by the alkali-metal counteranions. These cation-dependent properties are useful for selecting polyoxoanion precursor favorable to the crystallization of $P_2W_{15}Nb_3O_{62}^{9-}$ -supported organometallic complexes. The effects of the cations (Li, K, Na, and Cs) on the $P_2W_{15}Nb_3O_{62}^{9-}$ were observed as different hydrated structures of the polyoxoanion and its cation-dependent thermal stability in the solid state by a combination of TG/DTA and FT-IR measurements, and also as a spectral change of the downfield ^{31}P signal due to interactions of the polyoxoanion with the counteranions and/or with hydrated waters by variable-temperature (VT) solid-state GHD/MAS ^{31}P NMR spectroscopy.

Polyoxoanions are molecular metal-oxide clusters which resemble discrete fragments of solid metal oxides. Recently, we reported on the synthesis of the nonasodium salt of Dawson-type triniobium-substituted polyoxoanion B- α - $P_2W_{15}Nb_3O_{62}^{9-}$.^{1a)} That work was aimed at providing a water-soluble form of the important $P_2W_{15}Nb_3O_{62}^{9-}$ polyoxoanion (Fig. 1); prior to that work, the $P_2W_{15}Nb_3O_{62}^{9-}$ polyoxoanion had been available only as its organic solvent-soluble, but water-insoluble, nonakis (TBA) salt (TBA = [(*n*-C₄H₉)₄N]).^{1b)} Hence, the nonasodium salt of $P_2W_{15}Nb_3O_{62}^{9-}$ extended the well-documented organometallic chemistry of $P_2W_{15}Nb_3O_{62}^{9-}$ into aqueous media.^{1a)}

In a separate account, full details concerning the synthesis and isolation of a polyoxoanion-supported organometallic complex [$\{(\eta^5\text{-C}_5\text{Me}_5)\text{Rh}\}(P_2W_{15}Nb_3O_{62})\}^{7-}$] as its heptakis (TBA) salt were reported.^{1b,1d)} In this compound, the organometallic moiety, [$(\eta^5\text{-C}_5\text{Me}_5)\text{Rh}\}^{2+}$, is bonded to three bridging Nb₂O oxygens that cap the $P_2W_{15}Nb_3O_{62}^{9-}$ Dawson-type polyoxoanions, as shown by a single-crystal

X-ray diffraction analysis for its mixed (TBA)₆Na salt.^{1d)} Nevertheless, there exists a crystallization problem in the $P_2W_{15}Nb_3O_{62}^{9-}$ -supported organometallic complexes, e.g., the (TBA)₇ salt; even the mixed (TBA)_{7-x}Na_x salts of the supported (C₅Me₅)Rh²⁺ complex, soluble in organic solvents (e.g., CH₃CN, DMSO, and acetone) and insoluble in water, are hard to crystallize.

Very recently, it was realized that by using the nonasodium salt of $P_2W_{15}Nb_3O_{62}^{9-}$ the concept of water solubility and all-inorganic composition could be extended to [$\{(\eta^5\text{-C}_5\text{Me}_5)\text{Rh}\}(P_2W_{15}Nb_3O_{62})\}^{7-}$].^{1e)} The nonasodium salt of $P_2W_{15}Nb_3O_{62}^{9-}$ and the heptasodium salt of [$\{(\eta^5\text{-C}_5\text{Me}_5)\text{Rh}\}(P_2W_{15}Nb_3O_{62})\}^{7-}$] have never been derived by direct cation-metathesis from their TBA salts, but have been obtained by their own synthetic routes.^{1a,1e)} Also, as previously shown in heterogeneous catalysts using classical Keggin-type heteropolyanions, the amount of solvated water, and therefore the porosity, thermal stability and surface area, can be controlled by the use of different counteranions.²⁾

A clarification of the cation-dependent properties of the

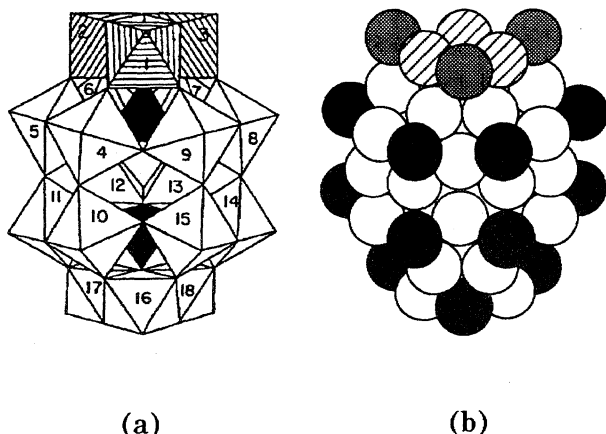


Fig. 1. (a) Polyhedral and (b) space-filling representation of the Dawson-type heteropolyanion α -1,2,3- $P_2W_{15}Nb_3O_{62}^{9-}$. In (a) the three niobiums are represented by hatched octahedra in the 1—3 positions. The WO_6 octahedra occupy the 4—18 positions and two PO_4 groups are shown as the internal, black tetrahedron. In (b) the open circles represent bridging tungsten oxygens (W_2O), while the black circles represent terminal tungsten oxygens (WO). Niobium bridging oxygens (Nb_2O) are depicted by hatched circles, whereas niobium terminal oxygens (NbO) are shown as gray circles. From the space-filling representation it becomes clear that heteropolyoxoanions are composed of a close-packed array of oxygens, and this representation, in turn, reveals their potential as a soluble metal oxide analog.

polyoxoanion helps to overcome the crystallization problem of the $P_2W_{15}Nb_3O_{62}^{9-}$ -supported organometallic complexes, and also to design novel types of solid-base heterogeneous catalysts.^{2,3)} Furthermore, the synthetic procedure described herein provides a general route to cation metathesis of polyoxoanion-supported complexes.^{1c,4)}

Herein we provide full details concerning the synthesis and isolation of the alkali metal salts of $P_2W_{15}Nb_3O_{62}^{9-}$ as its Li salt with 25 water (2), as its K salt with 9 water (1) and as its Cs salt with 8 water (3) under atmospheric conditions. We also give the characteristics of the polyoxoanion with these alkali metal salts, including the previously prepared Na salt (4). Also reported are the compositional characterization by full elemental analyses, thermogravimetric and differential thermal analyses (TG/DTA), and structural characterization by FT-IR and variable-temperature solid-state ^{31}P NMR as well as by solution ^{31}P and ^{183}W NMR spectroscopies at room temperature. The effects of alkali-metal counteranions on the thermal stability of $P_2W_{15}Nb_3O_{62}^{9-}$ were observed in the solid state by a combination of TG/DTA and FT-IR measurements; also observed was a change in the ^{31}P signal in the PO_4 moiety closer to the Nb_3O_6 site in the Dawson structure by using variable-temperature (VT) solid-state ^{31}P NMR spectroscopy.

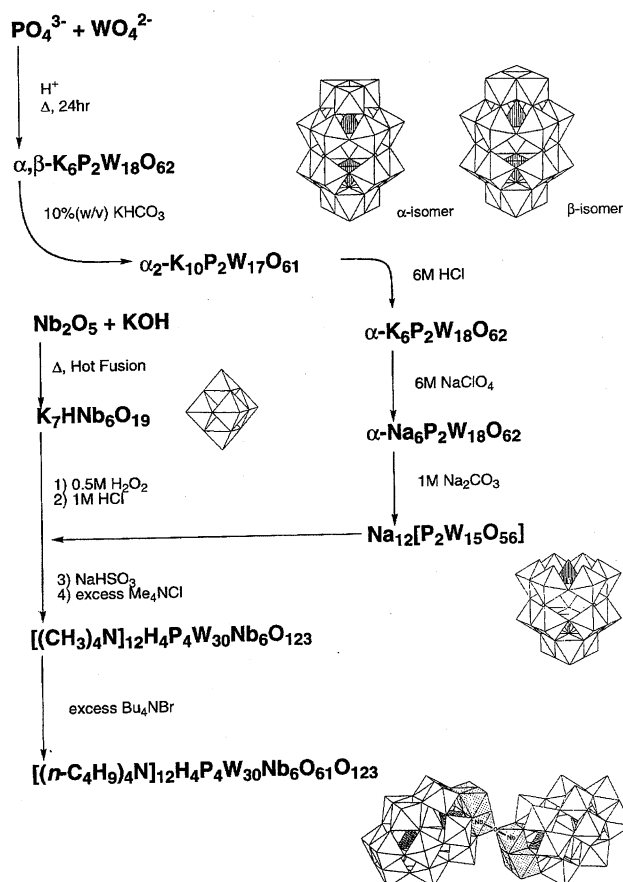
Experimental

General Conditions. The following were used as received: $LiClO_4$, KBF_4 , 0.5 M $LiOH$ (aq), 0.5 M KOH (aq), $CsOH$, $EtOAc$,

CH_3CN , $(CH_3)_2CO$, $(CH_3)_2SO$ (all from Wako) (1 M = 1 mol dm^{-3}); $LiBF_4$, $DMSO-d_6$ (Aldrich), and D_2O (Merck). Solid $CsBF_4$ was prepared in analogy with the synthesis of KBF_4 reported in the literature.^{5,6)} $[(n-C_4H_9)_4N]_{12}H_4P_4W_{30}Nb_6O_{123}$ was prepared as previously described,^{1c,1d)} via the 7 steps shown in Scheme 1.

Instrumentation and Analytical Procedures. Elemental analyses on samples dried overnight at room temperature under 10^{-3} — 10^{-4} Torr (1 Torr = 133.322 Pa) were carried out by Mikro-analytisches Labor Pascher (Remagen, Germany). Infrared spectra were recorded on a Nicolet 510 FT-IR spectrometer in KBr disks at room temperature. Thermogravimetric (TG) and differential thermal analyses (DTA) were carried out using a Seiko SSC 5000 TG/DTA 300 system and a Rigaku TG 8101D and TAS 300 data-processing system. TG/DTA measurements were run under air with a temperature ramp of $5^\circ C\ min^{-1}$ between 20 and $550^\circ C$.⁷⁾

Solution ^{31}P NMR (161.70 MHz) spectra were recorded at $22^\circ C$ in 5 mm o.d. tubes on a JEOL JNM-EX 400 FT-NMR spectrometer with a JEOL EX-400 NMR data-processing system, and were referenced to an external standard of 25% H_3PO_4 in H_2O in a sealed capillary. Chemical shifts were reported as negative for resonances upfield of H_3PO_4 ($\delta = 0$). Solution ^{183}W NMR (16.50 MHz) spectra were recorded at $22^\circ C$ in 10 mm o.d. tubes on a JEOL JNM-EX 400 FT-NMR spectrometer equipped with a JEOL NM-40T10L low-frequency tunable probe and a JEOL EX-400 NMR data-processing system. These spectra were referenced to an external standard of saturated Na_2WO_4 - D_2O solution by the substitution method. Chemical shifts were reported on the δ scale with resonances upfield of Na_2WO_4 ($\delta = 0$) as negative.



Scheme 1. Preparation of $[(n-C_4H_9)_4N]_{12}H_4P_4W_{30}Nb_6O_{123}$.

Solid-state ^{31}P NMR spectra were measured over a wide range of temperatures by high-resolution solid state NMR. Variable-temperature (VT) ^{31}P high-power proton decoupling (GHD)/magic angle spinning (MAS) NMR spectra were recorded over the temperature range 24 to 140 °C using a JEOL EX 270 spectrometer equipped with a VT GHD/MAS accessory operating at 109.25 MHz. The single 90° pulse (4.0 μs) in combination with GHD without cross-polarization was used to generate the spectra. A silicon nitride ceramic cylindrical-type rotor was used. Line narrowing was achieved by high-order decoupling and magic angle spinning. The spinning rate was set to about 6 kHz. A variable-temperature (VT) controller was used for all of the probe temperatures at which measurements were taken. The spectral width and data points were 54.3 kHz and 8 k, respectively. The spectra were usually accumulated 600–2000 times at a repetition time of 5 s to achieve a reasonable signal-to-noise ratio. The ^{31}P NMR chemical shifts were calibrated indirectly through external $(\text{NH}_4)_2\text{HPO}_4$ [1.6 ppm relative to H_3PO_4 ($\delta=0$)]. The experimental errors of the isotropic ^{31}P chemical shift values are estimated to be about 0.5 ppm. Spinning side bands did not appear due to a sufficient spinning rate.

Synthesis of $\text{K}_9\text{P}_2\text{W}_{15}\text{Nb}_3\text{O}_{62}\cdot 9\text{H}_2\text{O}$ (1). The present preparation is based on a major modification of the previously reported synthesis of $\text{Na}_9\text{P}_2\text{W}_{15}\text{Nb}_3\text{O}_{62}\cdot 23\text{H}_2\text{O}$ **4**^(a) by using KBF_4 and a 0.5 M aqueous KOH solution instead of NaBF_4 and a 0.5 M aqueous NaOH solution. The target compound was formed by a stoichiometric reaction in an aqueous/ CH_3CN system, and isolated by crystallization from a solution of unbuffered pH 8 water.

In a 300 mL beaker were placed 5.00 g (0.451 mmol) of $[(n\text{-C}_4\text{H}_9)_4\text{N}]_{12}\text{H}_4\text{P}_4\text{W}_{30}\text{Nb}_6\text{O}_{123}$ and 50 mL of CH_3CN . Warming the mixture to 50–60 °C and stirring resulted in a clear, pale-yellow solution. While the solution temperature was maintained at 50–60 °C, solid KBF_4 (0.681 g, 5.412 mmol, 12 equiv) was added, followed by stirring for 30 min, during which time all of the KBF_4 remained undissolved. To this warm suspension, the dropwise addition of 5.41 mL (2.71 mmol, 6 equiv) of a 0.5 M aqueous KOH solution resulted in the formation of a cloudy suspension containing white precipitates. After the addition of the base was completed, stirring was continued for an additional 20 min. (Separation of $\text{K}_9\text{P}_2\text{W}_{15}\text{Nb}_3\text{O}_{62}$ and $[(n\text{-C}_4\text{H}_9)_4\text{N}]\text{BF}_4$ from their mixture was accomplished by reprecipitation with CH_3CN . $[(n\text{-C}_4\text{H}_9)_4\text{N}]\text{BF}_4$ is soluble in CH_3CN , whereas the nonapotassium salt of heteropolyanion is not.) By the addition of 50 mL of CH_3CN to the reaction mixture, followed by stirring for 20 min in an ice-cooled bath, white precipitates were produced, which were collected on a medium glass frit, washed with CH_3CN (20 mL \times 3), then with 500 mL of ethyl acetate (unreacted KBF_4 is dissolved in a large excess of ethyl acetate), finally with ether (40 mL \times 2), and dried overnight in a 55 °C oven. Next, this crude precipitate was added to ca. 50 mL of unbuffered pH 8 water (the pH was adjusted with a diluted KOH aqueous solution) and redissolved by warming to 60 °C. The warm, cloudy solution was filtered through folded filter paper (Whatman No. 5), and the clear filtrate was rotary evaporated at 60 °C until it became slightly cloudy. This concentrated solution was cooled to room temperature and then placed in a refrigerator at 5 °C overnight. Colorless crystals resulted, which were dried in a 55 °C oven. At this stage, the ^{31}P NMR spectra of this crystalline compound measured in $\text{DMSO}-d_6$ at room temperature showed a signal at -8.6 ppm, probably due to the protonated species of the heteropolyoxoanion. Recrystallizations from unbuffered pH 8 water were repeated until no signal at -8.6 ppm in the ^{31}P NMR in $\text{DMSO}-d_6$ was detected. Analytically pure colorless crystals were obtained in 2.6 g yield (63%). The compound is soluble in water

and DMSO, but insoluble in CH_3CN and ethyl acetate.

Microanalysis. Analytical results for the sample dried overnight at room temperature under 10^{-3} – 10^{-4} Torr: Found: H, 0.30; K, 7.52; P, 1.46; W, 60.9; Nb, 6.05; O, 22.8%; Total 99.0%. Calcd for $\text{H}_6\text{K}_9\text{P}_2\text{W}_{15}\text{Nb}_3\text{O}_{65}$, or $\text{K}_9\text{P}_2\text{W}_{15}\text{Nb}_3\text{O}_{62}\cdot 3\text{H}_2\text{O}$: H, 0.13; K, 7.83; P, 1.38; W, 61.3; Nb, 6.20; O, 23.1%. TG/DTA done under atmospheric conditions: weight loss of 3.63% found with a temperature ramp of 5 °C min^{-1} below 500 °C with an endothermic point at 101 °C; calcd 3.52% for $x=9$ in $\text{K}_9\text{P}_2\text{W}_{15}\text{Nb}_3\text{O}_{62}\cdot x\text{H}_2\text{O}$. IR (KBr) (Fig. 2(c)) 1617m, 1086s, 1058w, 1015w, 945s, 913s, 765s, br, 527w cm^{-1} . ^{31}P NMR (D_2O , 23 °C) (Fig. 3(a)) $\delta = -7.7$ (1.0 P, $\Delta\nu_{1/2} = 2.3$ Hz), -14.3 (1.0 P, $\Delta\nu_{1/2} = 3.0$ Hz). ^{31}P NMR ($\text{DMSO}-d_6$, 23 °C) (Fig. 3(b)) $\delta = -7.8$ (1.0 P, $\Delta\nu_{1/2} = 3.3$ Hz); -14.3 (1.0 P, $\Delta\nu_{1/2} = 2.9$ Hz). ^{183}W NMR (D_2O , 45 °C) $\delta = -147.6$ (3W, $\Delta\nu_{1/2} = 2.7$ Hz), -173.2 (6W, $\Delta\nu_{1/2} = 5.6$ Hz), -216.1 (6W, $\Delta\nu_{1/2} = 3.4$ Hz). ^{183}W NMR (D_2O , 25 °C) measured for the solution obtained by cation-exchanging the potassium salt in D_2O with excess of LiClO_4 , followed by filtering off the KClO_4 : $\delta = -152.2$ (3W, $\Delta\nu_{1/2} = 2.9$ Hz); -177.9 (6W, $\Delta\nu_{1/2} = 4.8$ Hz), -220.0 (6W,

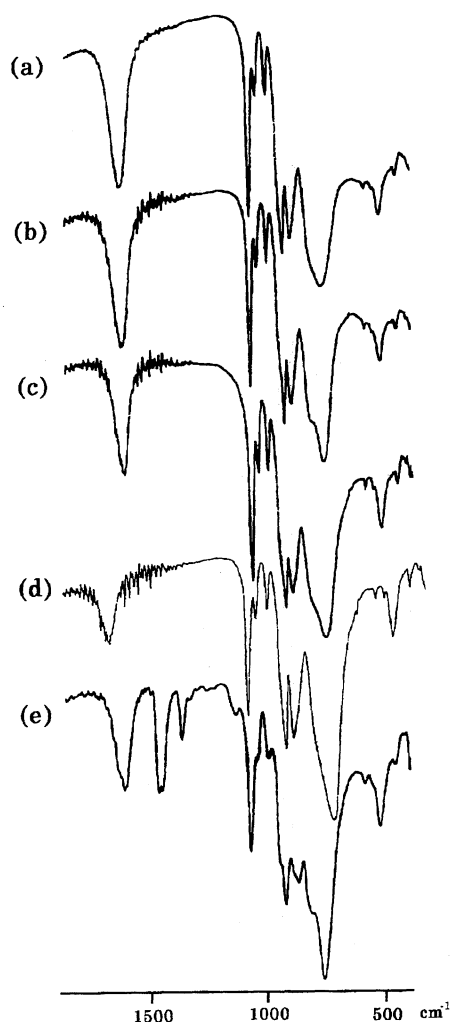


Fig. 2. The FT-IR spectra, measured as KBr disks of (a) $\text{Li}_9\text{P}_2\text{W}_{15}\text{Nb}_3\text{O}_{62}$ **2**, of (b) $\text{Na}_9\text{P}_2\text{W}_{15}\text{Nb}_3\text{O}_{62}$ **4**, of (c) $\text{K}_9\text{P}_2\text{W}_{15}\text{Nb}_3\text{O}_{62}$ **1**, of (d) $\text{Cs}_9\text{P}_2\text{W}_{15}\text{Nb}_3\text{O}_{62}$ **3**, and of (e) $[(n\text{-C}_4\text{H}_9)_4\text{N}]_9\text{P}_2\text{W}_{15}\text{Nb}_3\text{O}_{62}$ **5** demonstrating that the polyoxoanion regions of the IR of these salts are completely coincident.

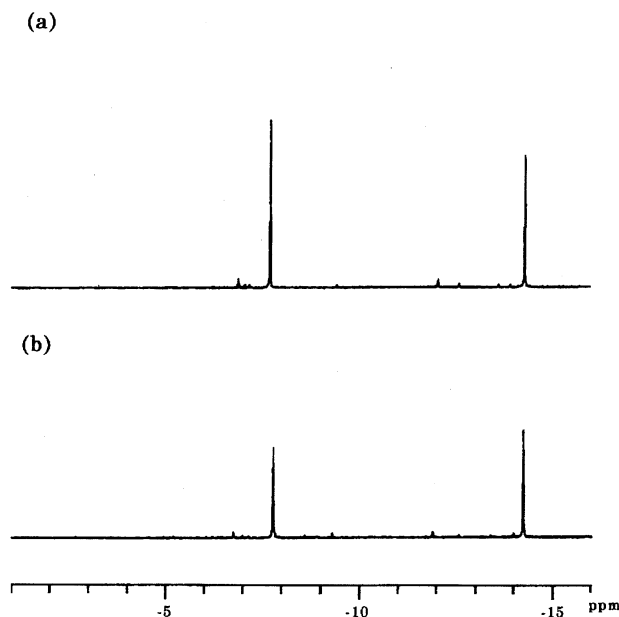


Fig. 3. Solution ^{31}P NMR spectra of $\text{K}_9\text{P}_2\text{W}_{15}\text{Nb}_3\text{O}_{62}$ 1 measured at 23 °C in (a) D_2O and (b) $\text{DMSO}-d_6$.

$\Delta\nu_{1/2} = 3.8$ Hz). ^{183}W NMR ($\text{DMSO}-d_6$, 23 °C) $\delta = -135.6$ (3W, $\Delta\nu_{1/2} = 14.0$ Hz), -161.2 (6W, $\Delta\nu_{1/2} = 9.8$ Hz), -201.8 (6W, $\Delta\nu_{1/2} = 16.1$ Hz). Solid-state ^{31}P NMR (Fig. 6) (26.4 °C) $\delta = -6.8$, -7.5 , -14.1 ($\Delta\nu_{1/2} = 46$ Hz). Solid-state ^{31}P NMR (60.0 °C) $\delta = -6.7$, -7.5 , -13.8 ($\Delta\nu_{1/2} = 92$ Hz). Solid-state ^{31}P NMR (80.0 °C) $\delta = -6.7$, -7.5 , -13.7 ($\Delta\nu_{1/2} = 108$ Hz). Solid-state ^{31}P NMR (120.0 °C) $\delta = -6.7$, -7.5 , -13.7 ($\Delta\nu_{1/2} = 139$ Hz). Solid-state ^{31}P NMR (140.0 °C) $\delta = -6.7$, -13.6 ($\Delta\nu_{1/2} = 146$ Hz). Solid-state ^{31}P NMR (the sample measured at 140.0 °C was cooled and remeasured at 25.6 °C) $\delta = -6.8$, -7.6 , -14.2 ($\Delta\nu_{1/2} = 131$ Hz).

Synthesis of $\text{Li}_9\text{P}_2\text{W}_{15}\text{Nb}_3\text{O}_{62} \cdot 25\text{H}_2\text{O}$ (2). Handling of the very hygroscopic LiBF_4 was performed in a glove box. The target compound was formed in an aqueous/ CH_3CN system and isolated by reprecipitation with excess acetone from a solution of unbuffered pH 8 water.

In a glove box, 0.305 g (3.25 mmol, 12 equiv) of solid LiBF_4 were added to 3.00 g (0.271 mmol) of $[(n\text{-C}_4\text{H}_9)_4\text{N}]_{12}\text{H}_4\text{P}_4\text{W}_{30}\text{Nb}_6\text{O}_{123}$ dissolved in 20 mL of CH_3CN in a 200 mL beaker. To the clear solution taken out from the glove box, 3.25 mL (1.63 mmol, 6 equiv) of a 0.5 M aqueous LiOH solution was added dropwise. After the stirring aqueous solution became cloudy, an oil precipitate formed. Stirring was continued for an additional 20 min. The supernatant was discarded by decantation. The colorless oil precipitate was changed to a dry powder by washing three times with ca. 10 mL CH_3CN . It was dried overnight in a 55 °C oven. The crude materials were redissolved in ca. 10 mL of unbuffered pH 8 water. The cloudy solution was filtered through filter paper (Whatman No. 5). To the clear colorless filtrate about 100–150 mL of acetone were added dropwise with stirring. The white precipitates were reprecipitated. The mother liquor was removed by decantation, and the precipitates were dried overnight in a 55 °C oven. The yield was 1.9 g (76%). The compound is very soluble in water, soluble in MeOH, EtOH, and DMSO and slightly soluble in CH_3CN , but insoluble in acetone and ethyl acetate.

Microanalysis. Analytical results for the sample dried overnight at room temperature under 10^{-3} – 10^{-4} Torr: Found: H, 0.28; Li, 1.55; P, 1.83; W, 63.6; Nb, 6.57; O, 26.0%; total 99.8%.

Calcd for $\text{H}_{18}\text{Li}_9\text{P}_2\text{W}_{15}\text{Nb}_3\text{O}_{71}$, or $\text{Li}_9\text{P}_2\text{W}_{15}\text{Nb}_3\text{O}_{62} \cdot 9\text{H}_2\text{O}$: H, 0.42; Li, 1.45; P, 1.44; W, 63.9; Nb, 6.46; O, 26.3%. TG/DTA done under atmospheric conditions: weight loss of 9.87% found with a temperature ramp of 5 °C min^{-1} below 400 °C with an endothermic point at 82 °C; calcd 9.78% for $x=25$ in $\text{Li}_9\text{P}_2\text{W}_{15}\text{Nb}_3\text{O}_{62} \cdot x\text{H}_2\text{O}$. IR (KBr) (Fig. 2(a)) 1631m, 1087s, 1059w, 1015w, 949s, 916s, 791s, br, 599w, 533s, 463w cm^{-1} . ^{31}P NMR (D_2O , 25 °C) (Fig. 4(a)) $\delta = -7.8$ (1.0 P, $\Delta\nu_{1/2} = 2.7$ Hz), -14.3 (1.0 P, $\Delta\nu_{1/2} = 3.0$ Hz). ^{31}P NMR ($\text{MeOH}-d_4$, 25 °C) (Fig. 4(c)) $\delta = -7.2$ (1.0 P, $\Delta\nu_{1/2} = 2.2$ Hz), -13.6 (1.0 P, $\Delta\nu_{1/2} = 2.7$ Hz). ^{31}P NMR ($\text{DMSO}-d_6$, 25 °C) (Fig. 4(b)) $\delta = -7.1$ (1.0 P, $\Delta\nu_{1/2} = 3.1$ Hz), -14.0 (1.0 P, $\Delta\nu_{1/2} = 2.3$ Hz); δ [minor peak] = -4.0 ($\Delta\nu_{1/2} = 4.4$ Hz), -10.0 ($\Delta\nu_{1/2} = 4.4$ Hz). ^{183}W NMR (Fig. 5) (D_2O , 25 °C) $\delta = -152.4$ (3W, $\Delta\nu_{1/2} = 3.6$ Hz), -178.1 (6W, $\Delta\nu_{1/2} = 4.9$ Hz), -220.3 (6W, $\Delta\nu_{1/2} = 3.8$ Hz). ^{183}W NMR ($\text{MeOH}-d_4$, 25 °C) $\delta = -159.1$ (3W, $\Delta\nu_{1/2} = 4.9$ Hz), -188.5 (6W, $\Delta\nu_{1/2} = 5.6$ Hz), -232.0 (6W, $\Delta\nu_{1/2} = 4.7$ Hz). ^{183}W NMR ($\text{DMSO}-d_6$, 25 °C) $\delta = -137.1$ (3W, $\Delta\nu_{1/2} = 17.8$ Hz), -161.7 (6W, $\Delta\nu_{1/2} = 10.8$ Hz), -214.4 (6W, $\Delta\nu_{1/2} = 12.7$ Hz); δ [minor peak] = -199.8 ($\Delta\nu_{1/2} = 8.5$ Hz). Solid-state ^{31}P NMR (Fig. 6) (27.3 °C) $\delta = -6.8$, -8.0 , -14.3 ($\Delta\nu_{1/2} = 185$ Hz). Solid-state ^{31}P NMR (60.0 °C) $\delta = -6.7$, -7.9 , -14.2 ($\Delta\nu_{1/2} = 185$ Hz). Solid-state ^{31}P NMR (80.0 °C) $\delta = -6.7$, -7.9 , -14.1 ($\Delta\nu_{1/2} = 177$ Hz). Solid-state ^{31}P NMR (100.0 °C) $\delta = -6.7$, -7.9 , -13.9 ($\Delta\nu_{1/2} = 180$ Hz). Solid-state ^{31}P NMR (120.0 °C) $\delta = -6.7$, -7.9 ,

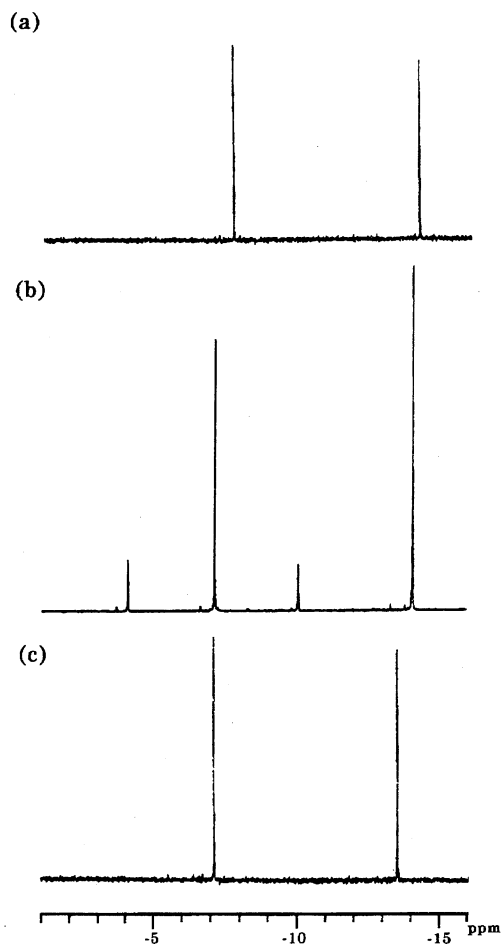


Fig. 4. Solution ^{31}P NMR spectra of $\text{Li}_9\text{P}_2\text{W}_{15}\text{Nb}_3\text{O}_{62}$ 2 measured at 25 °C in (a) D_2O , (b) $\text{DMSO}-d_6$, and (c) $\text{MeOH}-d_4$.

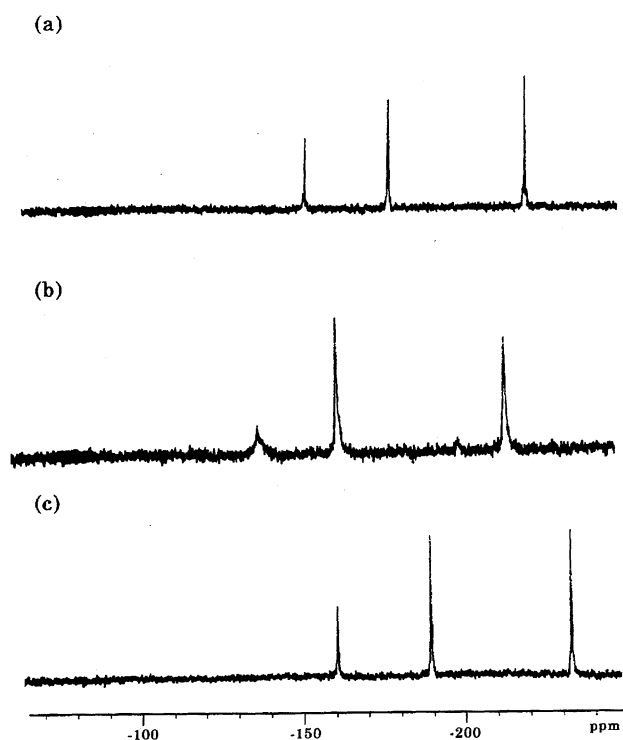


Fig. 5. Solution ^{183}W NMR of $\text{Li}_9\text{P}_2\text{W}_{15}\text{Nb}_3\text{O}_{62}$ **2** measured at 25 °C in (a) D_2O , (b) $\text{DMSO}-d_6$, and (c) $\text{MeOH}-d_4$.

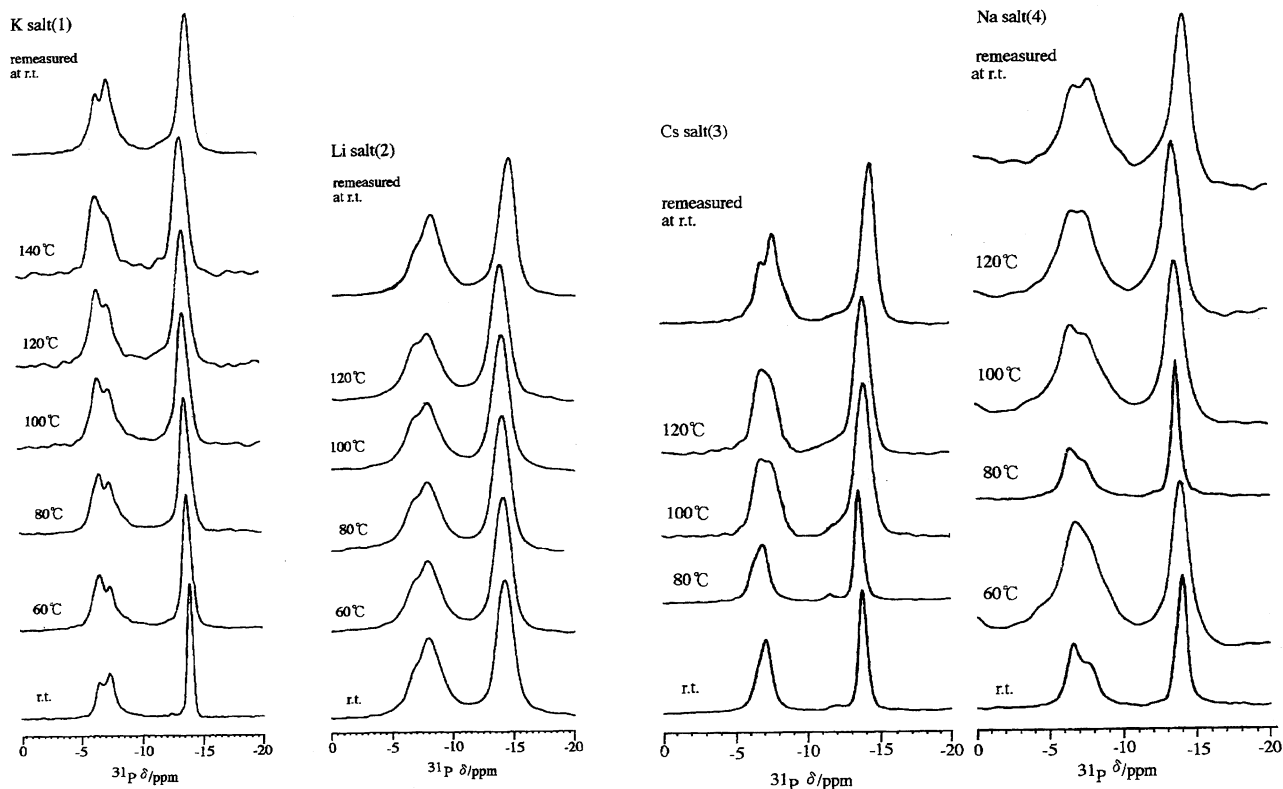


Fig. 6. Variable-temperature solid-state GHD/MAS ^{31}P NMR spectra of $\text{K}_9\text{P}_2\text{W}_{15}\text{Nb}_3\text{O}_{62}$ **1**, $\text{Li}_9\text{P}_2\text{W}_{15}\text{Nb}_3\text{O}_{62}$ **2**, $\text{Cs}_9\text{P}_2\text{W}_{15}\text{Nb}_3\text{O}_{62}$ **3**, and $\text{Na}_9\text{P}_2\text{W}_{15}\text{Nb}_3\text{O}_{62}$ **4**. In these spectra, after the sample was cooled from the highest temperature, the top spectrum was remeasured at room temperature.

−13.7 ($\Delta\nu_{1/2}$ = 185 Hz). Solid-state ^{31}P NMR (the sample measured at 120 °C was cooled and remeasured at 27.0 °C) δ = −6.8, −8.0, −14.3 ($\Delta\nu_{1/2}$ = 170 Hz).

In a separate, unsuccessful attempt, the isolation of the solid Li_9 salt by cation-exchange from the K_9 salt using an excess of LiClO_4 failed. The precipitate obtained by reprecipitation with excess acetone was insoluble in MeOH and EtOH, and the ^{31}P NMR in $\text{DMSO}-d_6$ showed a two-line spectrum, δ = −7.7 and −14.1 ppm. The compound obtained in this way was probably a mixed-counteranion (K, Li) $_9$ species.

Synthesis of $\text{Cs}_9\text{P}_2\text{W}_{15}\text{Nb}_3\text{O}_{62} \cdot 8\text{H}_2\text{O}$ (3**).** The target compound was formed in an aqueous/DMSO system and isolated by reprecipitation from unbuffered pH 8 water at 90 °C.

In a 200 mL beaker were placed 5.00 g (0.451 mmol) of $[(n\text{-C}_4\text{H}_9)_4\text{N}]_{12}\text{H}_4\text{P}_4\text{W}_{30}\text{Nb}_6\text{O}_{123}$ and 80 mL of DMSO. Stirring resulted in a clear pale-yellow solution. Solid CsBF_4 (1.19 g, 5.41 mmol, 12 equiv) was added, followed by stirring for 60 min, during which time all of the CsBF_4 completely dissolved. To this clear pale-yellow solution, the dropwise addition of 5.41 mL (2.71 mmol, 6 equiv) of a 0.5 M aqueous CsOH solution resulted in the formation of a cloudy suspension containing white precipitates. After the addition of the base was completed, stirring was continued for an additional 1 h, during which the cloudy suspension became white. With centrifuging, the white precipitates settled at the bottom of the centrifuge tube. The slightly cloudy supernatant solution was discarded by decantation, the white precipitates were washed with ca. 20 mL DMSO, and the suspension was centrifuged again. (The filtration of the white precipitates with fine glass frit or fine filter paper is difficult, because of the excessively fine powder, and resulted in lower yields.) This work-up was repeated once more, during

which time unreacted $CsBF_4$ was completely removed. Next, the white precipitates were washed with ca. 30 mL CH_3CN , and then centrifuged. This work-up was carried out for a total of five times. The final precipitates were dried overnight in a 55 °C oven. The white powder was dissolved in 150 mL of unbuffered pH 8 water at 90 °C. The cloudy solution was passed through filter paper (Whatman No. 5). The clear colorless filtrate was placed in a refrigerator at 5 °C overnight. The compound, a colorless powder, was collected on a medium glass frit, thoroughly dried by suction, and dried overnight in a 55 °C oven. An analytically pure, colorless powder was obtained in 2.3 g yield (47%). The compound was soluble in hot water and a large amount of hot DMSO, but insoluble in MeOH, EtOH, CH_3CN , DMF, and ethyl acetate.

Microanalysis. Analytical results for the sample dried overnight at room temperature under 10^{-3} – 10^{-4} Torr: Found: H, 0.03; Cs, 21.6; P, 1.12; W, 51.8; Nb, 5.14; O, 19.7%; total 99.4%. Calcd for $H_6Cs_9P_2W_{15}Nb_3O_{65}$, or $Cs_9P_2W_{15}Nb_3O_{62} \cdot 3H_2O$: H, 0.11; Cs, 22.4; P, 1.16; W, 51.6; Nb, 5.22; O, 19.5%. TG/DTA done under atmospheric conditions: weight loss of 2.76% found with a temperature ramp of 5 °C min⁻¹ below 378 °C with an endothermic point at 154 °C; calcd 2.65% for $x = 8$ in $Cs_9P_2W_{15}Nb_3O_{62} \cdot xH_2O$. IR (KBr) (Fig. 2(d)) 1618m, 1086s, 1059w, 1014w, 944s, 913s, 768s, br, 598w, 564w, 530m, 462w cm⁻¹. ³¹P NMR (D_2O , 70 °C) $\delta = -7.4$ (1.0 P, $\Delta\nu_{1/2} = 2.2$ Hz), -13.9 (1.0 P, $\Delta\nu_{1/2} = 2.7$ Hz). ³¹P NMR (DMSO-*d*₆, 23 °C) $\delta = -7.7$ (1.0 P, $\Delta\nu_{1/2} = 5.8$ Hz), -14.4 (1.0 P, $\Delta\nu_{1/2} = 4.6$ Hz). Solid-state ³¹P NMR (Fig. 6) (25.4 °C) $\delta = -7.4$ ($\Delta\nu_{1/2} = 138$ Hz), -14.1 ($\Delta\nu_{1/2} = 108$ Hz). Solid-state ³¹P NMR (80.0 °C) $\delta = -6.8$, -7.5 , -13.9 ($\Delta\nu_{1/2} = 139$ Hz). Solid-state ³¹P NMR (100.0 °C) $\delta = -6.8$ ($\Delta\nu_{1/2} = 108$ Hz), -13.9 ($\Delta\nu_{1/2} = 139$ Hz). Solid-state ³¹P NMR (120.0 °C) $\delta = -6.9$ ($\Delta\nu_{1/2} = 216$ Hz), -13.9 ($\Delta\nu_{1/2} = 139$ Hz). Solid-state ³¹P NMR (the sample measured at 120.0 °C was cooled and remeasured at 25.5 °C) $\delta = -6.9$, -7.6 , -14.4 ($\Delta\nu_{1/2} = 123$ Hz).

A separate, unsuccessful attempt to isolate the solid Cs_9 salt by a cation-exchange from the K_9 salt using excess of $CsClO_4$ failed. A preparation based on a stoichiometric reaction in an aqueous/ CH_3CN system and precipitation from a solution of unbuffered pH 8 water at 90 °C gave a compound which showed the ³¹P NMR in D_2O at 70 °C major peaks at -7.4 and -14.0 ppm and minor peaks at -9.1 and -13.6 ppm, probably due to contamination of the starting dimeric compound, $P_4W_{30}Nb_6O_{123}$ ¹⁶⁻.

Synthesis of $Na_9P_2W_{15}Nb_3O_{62} \cdot 23H_2O$ (4). This compound was previously prepared and fully characterized in the form with 23 water;^{1a)} the crystal structure of the form containing 2 CH_3CN solvated and 23 water has already been determined by single-crystal X-ray diffraction.^{1b)} Here, the compound prepared according to the previously reported method^{1a)} was recharacterized in order to compare the properties of compounds **1**–**3** under the same conditions. The amount of water of hydration under atmospheric conditions, found previously,^{1a)} was reproducible.

Microanalysis. Analytical results for the sample dried overnight at room temperature under 10^{-3} – 10^{-4} Torr: Found: H, 0.09; Na, 4.73; P, 1.37; W, 62.9; Nb, 6.34; O, 24.0%; total 99.4%. Calcd for $H_8Na_9P_2W_{15}Nb_3O_{66}$, or $Na_9P_2W_{15}Nb_3O_{62} \cdot 4H_2O$: H, 0.18; Na, 4.74; P, 1.42; W, 63.1; Nb, 6.38; O, 24.2%. TG/DTA done under atmospheric conditions:⁷⁾ weight loss of 9.20% found below 500 °C with endothermic points at 84, 130 and 137 °C; calcd 8.79% for $x = 23$ in $Na_9P_2W_{15}Nb_3O_{62} \cdot xH_2O$. Solid-state ³¹P NMR (Fig. 6) (26.6 °C) $\delta = -7.0$ ($\Delta\nu_{1/2} = 173$ Hz), -14.3 ($\Delta\nu_{1/2} = 96$ Hz). Solid-state ³¹P NMR (60.0 °C) $\delta = -6.7$ ($\Delta\nu_{1/2} = 177$ Hz), -13.9 ($\Delta\nu_{1/2} = 154$ Hz). Solid-state ³¹P NMR (80.0 °C) $\delta = -6.5$, -7.7 , -13.9 ($\Delta\nu_{1/2} = 154$ Hz). Solid-state ³¹P NMR (100.0 °C) $\delta = -6.5$,

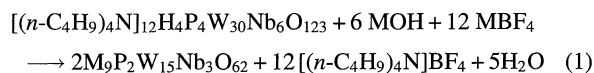
-7.6 , -13.8 ($\Delta\nu_{1/2} = 162$ Hz). Solid-state ³¹P NMR (120.0 °C) $\delta = -6.7$, -7.7 , -13.7 ($\Delta\nu_{1/2} = 170$ Hz). Solid-state ³¹P NMR (the sample measured at 120.0 °C was cooled and remeasured at 26.9 °C) $\delta = -6.7$, -7.9 , -14.2 ($\Delta\nu_{1/2} = 154$ Hz).

Separately, this compound was successfully obtained by a reaction in CH_3CN of the monomeric precursor $[(n-C_4H_9)_4N]_5H_4P_2W_{15}Nb_3O_{62}$, which was prepared using a recently found, improved method without any synthetic work-ups of the dimer $[(n-C_4H_9)_4N]_{12}H_4P_4W_{30}Nb_6O_{123}$,^{1b)} with 5 equiv of $NaBF_4$ and subsequent with 4 equiv of NaOH, followed by repeated reprecipitations from unbuffered pH 8 water with excess CH_3CN .^{1j)}

Results and Discussion

Synthetic Reactions, General Properties, and Compositions.

The alkali-metal salts of the Dawson-type heteropolyoxoanion $P_2W_{15}Nb_3O_{62}^{9-}$ have been formed by a stoichiometric reaction of the organic solvent-soluble, dimeric precursor $[(n-C_4H_9)_4N]_{12}H_4P_4W_{30}Nb_6O_{123}$ with MBF_4 and MOH ($M = Li, K$, and Cs), as follows:



The key points in the syntheses of $M_9P_2W_{15}Nb_3O_{62}$ ($M = Li, K, Cs$) are as follows: (a) the use of stoichiometric amounts (12 equiv) of MBF_4 ($M = Li, K, Cs$) to allow for an exchange of the 12 $[(n-C_4H_9)_4N]^+$ counteranions of the dimeric, organic solvent-soluble precursor, $[(n-C_4H_9)_4N]_{12}H_4P_4W_{30}Nb_6O_{123}$; (b) the use of DMSO as a solvent in, especially, the synthesis of Cs^+ salt, otherwise, $CsBF_4$ was not exchanged to $[(n-C_4H_9)_4N]^+$ counteranions; (c) the use of a total of 6 equiv of MOH ($M = Li, K, Cs$) to react with the four protons in the dimer (requiring 4 equiv of OH^-) and to hydrolytically cleave the bridging Nb–O–Nb bond (requiring an additional 2 equiv of OH^- and forming two H_2O); and (d) the removal of $[(n-C_4H_9)_4N]BF_4$ as a byproduct from the reaction mixture and purification to give analytically pure white solids by reprecipitation with excess amounts of acetone or recrystallization from a hot aqueous system of unbuffered pH 8 water.

The molecular formula of K_9 (**1**), Li_9 (**2**), Cs_9 (**3**), and Na_9 (**4**) salts, with 3 water, 9 water, 3 water, and 4 water, respectively, are based on complete elemental analyses performed for samples dried overnight at room temperature under 10^{-3} – 10^{-4} Torr (all elements, including oxygen, 99.0, 99.8, 99.4, and 99.4% totals are observed; see the Experimental section). On the other hand, TG/DTA measurements performed under atmospheric conditions show the presence of 9 water for **1**, 25 water for **2**, 8 water for **3**, and 23 water for **4**, respectively. The TG data estimates the apparent amount of water both intrinsic hydrated water and adsorbed water, via the weight loss observed between 20 and 500 °C. The DTA curves clearly show the presence of intrinsic hydrated water as endothermic peaks at 101 °C for **1**, 82 °C for **2**, 154 °C for **3**, and 84, 130, and 137 °C for **4**. Thus, each of the following can be significantly affected by counteranions: the amounts of hydrated water and adsorbed water, solubilities in water and in organic solvents, and ease of crystallization.

Infrared Spectra and Thermal Analysis. Infrared spectra (Fig. 2(a)—Fig. 2(e)) of the compounds **1**—**4** and of the previously obtained $[(n\text{-C}_4\text{H}_9)_4\text{N}]_9$ salt **5**^{1a)} show the presence of the characteristic Dawson-type polyoxoanion IR bands between 1100 and 700 cm^{-1} . In the spectrum shown in Fig. 2(e), the very intense C—H vibrations of the $[(n\text{-C}_4\text{H}_9)_4\text{N}]^+$ counteranions are observed at 1486—1381 cm^{-1} . These observations demonstrate that the Dawson-type, “ $\text{P}_2\text{W}_{18}\text{O}_{62}^{9-}$ ” heteropolytungstate framework remains intact under the synthesis conditions.⁸⁾

The effect of alkali-metal cations on the $\text{P}_2\text{W}_{15}\text{Nb}_3\text{O}_{62}^{9-}$ thermal-stability was observed in the solid state. Exothermic peaks without an accompanying weight loss were observed at different temperatures at around 500 °C with alkali metal ions: 473 °C for the Li salt **2**, 492 °C for the Na salt **4**, 529 °C for the K salt **1**, and 534 °C for the Cs salt **3**. FT-IR measurements after the samples were heated above such exothermic temperatures (up to ca. 550 °C) showed that the Dawson structure of the polyoxoanion was not maintained. Thus, the polyoxoanions degradate or decompose above these exothermic temperatures; such temperatures indicate the following order of relative thermal stability of the polyoxoanions with different cations: Cs salt **3** > K salt **1** > Na salt **4** > Li salt **2**.

Solution ^{31}P and ^{183}W NMR Spectra. Further solution characterization relied on multinuclear ^{31}P and ^{183}W NMR (Table 1 and Table 2). A ^{31}P NMR spectrum measured at 23 °C of $\text{K}_9\text{P}_2\text{W}_{15}\text{Nb}_3\text{O}_{62}$ **1** in D_2O (Fig. 3) shows primarily two resonances at $\delta = -7.7$ and -14.3 ppm with integrated intensities of 1 : 1, as expected for the two types of phosphorus present, and as previously observed in $\text{Na}_9\text{P}_2\text{W}_{15}\text{Nb}_3\text{O}_{62}$ **4** in D_2O at 22 °C ($\delta = -7.8$ and -14.3).^{1a)} The downfield

resonance ($\delta = -7.7$) is assigned to the phosphorus closest to the Nb_3O_6 site, whereas the upfield resonance at $\delta = -14.3$ is known to be due to the phosphorus closer to the W_3O_6 cap (Fig. 1). The two-line ^{31}P NMR spectrum (Fig. 3) requires the presence of a single species in solution, and, therefore, precludes the existence of even minor impurities. The clean, two-line ^{31}P NMR spectrum of **1** was also observed in a $\text{DMSO}-d_6$ solution at 23 °C, although their chemical shifts were very slightly altered ($\delta = -7.8$ and -14.3). A ^{31}P NMR spectrum of $\text{Cs}_9\text{P}_2\text{W}_{15}\text{Nb}_3\text{O}_{62}$ **3** with low solubility in water was measured at 70 °C in D_2O to show a clean two-line spectrum at $\delta = -7.4$ and -13.9 ppm due to a single species present. On the other hand, the ^{31}P NMR spectra (Fig. 4) of $\text{Li}_9\text{P}_2\text{W}_{15}\text{Nb}_3\text{O}_{62}$ **2**, at 25 °C in D_2O and in $\text{MeOH}-d_4$ showed the two-line spectra at ($\delta = -7.8$ and -14.3) and at ($\delta = -7.2$ and -13.6), respectively, whereas that measured at 25 °C in $\text{DMSO}-d_6$ (Fig. 4(b)) showed two sets of major peaks at $\delta = -7.1$ and -14.0 with 1 : 1 intensities and minor peaks at $\delta = -4.0$ and -10.0 ppm with equal intensities. With the addition of $\text{MeOH}-d_4$, only the minor peaks disappeared as the amount of $\text{MeOH}-d_4$ increased. The ^{31}P NMR spectral pattern, two sets of two-line spectra in the $\text{DMSO}-d_6$ solution of **2**, is quite different from that previously observed in $\text{DMSO}-d_6$ solutions of mixed salts, such as $[(n\text{-C}_4\text{H}_9)_4\text{N}]_5\text{Na}_3[\{(\text{cod})\text{Ir}\}(\text{P}_2\text{W}_{15}\text{Nb}_3\text{O}_{62})]$.^{1g,1h)} In the latter spectrum, only the ^{31}P resonance of the PO_4 moiety closer to the Nb_3O_6 site in the Dawson structure has been observed as a line-broadened signal, flanked by two smaller peaks, which were caused by ion-pairing interactions between Na^+ and $\text{P}_2\text{W}_{15}\text{Nb}_3\text{O}_{62}^{9-}$. In contrast to other cation salts, the results from **2** suggest that a molecular species or adduct

Table 1. Comparison of the Chemical Shifts in Solution and Solid-State ^{31}P NMR Spectra Reported for $\text{M}_9\text{P}_2\text{W}_{15}\text{Nb}_3\text{O}_{62}$ (M=Li, Na, K, Cs)

	δ (D_2O)	δ ($\text{DMSO}-d_6$)	δ ($\text{MeOH}-d_4$)	δ (Solid-state) ^{c)}
$\text{Li}_9\text{P}_2\text{W}_{15}\text{Nb}_3\text{O}_{62}$ 2 ^{b)}	-7.8, -14.3	-7.1, -14.0 (-4.00, -10.0)*	-7.2, -13.6	-6.8, -8.0, -14.3
$\text{Na}_9\text{P}_2\text{W}_{15}\text{Nb}_3\text{O}_{62}$ 4 ^{a)}	-7.8, -14.3	-7.6, -14.1	—	-7.0, -14.3
$\text{K}_9\text{P}_2\text{W}_{15}\text{Nb}_3\text{O}_{62}$ 1 ^{b)}	-7.7, -14.3	-7.8, -14.3	—	-6.8, -7.5, -14.1
$\text{Cs}_9\text{P}_2\text{W}_{15}\text{Nb}_3\text{O}_{62}$ 3 ^{b)}	-7.4, -13.9	-7.7, -14.4	—	-7.4, -14.1

a) Ref. 1a. b) This work. The solution NMR data of Li, Na, and K salts were obtained at 23 °C and those of the less soluble Cs salt at 70 °C. c) This work. Measurements were performed at room temperature. *) Minor peaks.

Table 2. Comparison of the Chemical Shifts in Solution ^{183}W NMR Spectra Reported for $\text{M}_9\text{P}_2\text{W}_{15}\text{Nb}_3\text{O}_{62}$ (M=Li, Na, K, Cs)

	δ (D_2O)	δ ($\text{DMSO}-d_6$)	δ ($\text{MeOH}-d_4$)
$\text{Li}_9\text{P}_2\text{W}_{15}\text{Nb}_3\text{O}_{62}$ 2 ^{b)}	-152.4, -178.1, -220.3	-137.1, -161.7, (-199.8)*, -214.4	-159.1, -188.5, -232.0
$\text{Na}_9\text{P}_2\text{W}_{15}\text{Nb}_3\text{O}_{62}$ 4 ^{a)}	-151.6, -177.2, -219.8	-137.4, -163.5, -206.9	—
$\text{K}_9\text{P}_2\text{W}_{15}\text{Nb}_3\text{O}_{62}$ 1 ^{b)}	-147.6, -173.2, -216.1	-135.6, -161.2, -201.8	—
$\text{Cs}_9\text{P}_2\text{W}_{15}\text{Nb}_3\text{O}_{62}$ 3 ^{b)}	—	—	—

a) Ref. 1a. b) This work. The data for the Li salt were obtained from measurements at 23 °C and those for the K salt at 45 °C. *) Minor peak.

formed between **2** and DMSO molecules is present in neat DMSO solvent.

The ^{183}W NMR spectrum measured at 45 °C for the K_9 salt **1** in D_2O shows three peaks at $\delta = -147.6$, -173.2 , and -216.1 ppm with integrated intensities of 1 : 2 : 2. This spectral pattern is in accord with the presence of two tungsten belts consisting of six WO_6 octahedra each and a tungsten cap of three WO_6 octahedra, as is expected for a Wells–Dawson heteropolyanion (Fig. 1). The three-line ^{183}W NMR spectrum also requires that the heteropolyanion as a single species has an overall C_{3v} symmetry. The three-line ^{183}W NMR was also observed in a $\text{DMSO}-d_6$ solution. The ^{183}W NMR of the Cs_9 salt **3** was not measured in D_2O or in $\text{DMSO}-d_6$, because of its low solubility, even at elevated temperature. The 25 °C ^{183}W NMR spectra (Fig. 5, Table 2) of the Li_9 salt **2**, both in D_2O and in $\text{MeOH}-d_4$, also showed typical three-line spectra with integrated intensities of 1 : 2 : 2 (at $\delta = -152.4$, -178.1 , -220.3 , and at $\delta = -159.1$, -188.5 , -232.0 , respectively). On the other hand, the ^{183}W NMR (Fig. 5(b)) of **2** in $\text{DMSO}-d_6$ at 25 °C showed a minor broad peak at $\delta = -199.8$ in addition to the three-line spectrum consisting of major peaks at $\delta = -137.1$, -161.7 , and -214.4 . The $\delta = -137.1$ peak among the major peaks is specially broadened, and all of the major peaks are much more shifted to the downfield. In correlation to the minor two-line ^{31}P NMR spectrum observed in $\text{DMSO}-d_6$, the minor peak observed at $\delta = -137.1$ may be a part of the “three-line spectrum” of the new species or adduct formed between **2** and DMSO molecules in neat DMSO solvent, because the other two minor peaks are possibly obscured by the major peaks. Thus, only the Li_9 salt shows the cation effect in DMSO solution as an adduct formation between **2** and DMSO molecules.

Solid-State GHD/MAS ^{31}P NMR Spectra. Variable-temperature solid-state GHD/MAS ^{31}P NMR spectra of the polyoxoanions with different cations **1–4** are shown in Fig. 6, and their chemical shifts at room temperature listed in Table 1. Solid-state MAS ^{31}P NMR spectra, consisting of the much broader, or split, downfield signal and the upfield signal as a single peak, are significantly different from the spectral pattern observed in the solution ^{31}P NMR spectra, although both the solid-state and solution ^{31}P NMR spectra correspond. Therefore, the downfield signal can then be assigned to the phosphorus closer to the Nb_3O_6 site and the upfield signal to the phosphorus closer to the W_3O_6 Site.

The solid-state ^{31}P NMR of the K salt **1** at room temperature has three distinct resonances consisting of two split broad downfield peaks ($\delta = -6.8$ and -7.5 ; their separation is $\Delta\delta = 0.7$) and one major upfield peak ($\delta = -14.1$). As the temperature was elevated (from room temperature to 140 °C), the intensity of the -6.8 ppm signal gradually increased, compared to that of the -7.5 ppm signal, with only a slight shift of their chemical shifts downfield, and both signals coalesced around 140 °C. The upfield signal at -14.1 ppm as a single peak was also shifted downfield and broadened as the temperature increased. The sample measured at 140 °C was cooled, and then remeasured at room temperature. The resulting spectrum was almost the original spectral pat-

tern, i.e., the chemical shift of the upfield signal returned to the original position and the splitting of the downfield signal appeared again, although the relative intensity of the -6.8 and -7.5 ppm signals were slightly different from that of the starting spectrum.

It was previously found in solid-state ^{31}P NMR measurements of the $\text{H}_3\text{PW}_{12}\text{O}_{40} \cdot n\text{H}_2\text{O}$ that the solid-state ^{31}P resonances reflect the number of hydrated water interacting with the polyoxoanion.^{9a)} Some of water molecules were removed from the hydrated structures of the present polyoxoanion by elevating the temperature; the dehydrating behavior was dependent on the counteraction, as observed in the TG/DTA measurements (see the Experimental section for details). Thus, the solid ^{31}P NMR spectra of the K salt **1** indicate there exist at least two types of hydrated structures of the polyoxoanion, even at room temperature: one is the much more dehydrated species assignable to the $\delta = -6.8$ ppm signal; the other is the more hydrated species assignable to the $\delta = -7.5$ ppm signal, although such species can not be definitely distinguished in the upfield signal. The spectrum remeasured at room temperature, after the sample was heated up to 140 °C, indicates that the partial rehydration of the dehydrated species formed during heating takes place with the moisture in air.

In the solid-state ^{31}P NMR spectra of other salts at elevated temperature, the temperature-depending behavior of both the downfield and upfield signals appears to be similar to that of the K salt, although the splitting of the downfield signal is not clear compared with that of the K salt. Also, in other salts, the effect of the counteraction is most clearly observed in the change of the downfield signal with elevated temperature.

In the solid-state MAS ^{31}P NMR spectrum of the $\alpha\text{-P}_2\text{W}_{18}\text{O}_{62}^{6-}$ polyoxoanion with D_{3h} symmetry, the isotropic chemical shift has been observed at -13 ± 0.2 ppm as a single peak.^{9d)} Thus, the observation of the VT solid-state ^{31}P NMR as a function of different counteractions should consider intercalations of the $\alpha\text{-P}_2\text{W}_{15}\text{Nb}_3\text{O}_{62}^{9-}$ polyoxoanion with the counteractions and/or with hydrated water.

As for the fact that the downfield signal, rather than the upfield signal, is markedly effected by the counteraction, we can discuss at least two effects, which apparently cause the inhomogeneities of the polyoxoanion in the crystals⁹⁾ and have never been seen in an aqueous solution. One is a solid-state ion-pairing effect formed between the alkali metal cation and the Nb_3O_6 cap site of the $\text{P}_2\text{W}_{15}\text{Nb}_3\text{O}_{62}^{9-}$ polyoxoanion; the other is a dependence of the cation on the removal of the hydrated water from the crystal lattice at elevated temperature. The former effect is supported by single-crystal X-ray crystallography of the Na salt **4**,^{1f)} (described below); the latter effect is supported by the cation-dependent weight losses accompanying the different endothermic peaks, observed in the TG/DTA measurements.

The structure of $\alpha\text{-P}_2\text{W}_{15}\text{Nb}_3\text{O}_{62}^{9-}$ polyoxoanion has been determined by X-ray analysis for the single crystal of $\text{Na}_9\text{P}_2\text{W}_{15}\text{Nb}_3\text{O}_{62} \cdot 2\text{CH}_3\text{CN} \cdot 23\text{H}_2\text{O}$,^{1f)} two molecules are present in the unit cell. The crystals contain Na^+ and $\text{P}_2\text{W}_{15}\text{Nb}_3\text{O}_{62}^{9-}$ ions and CH_3CN and H_2O solvated

molecules. In the crystals, the cations are distributed fairly uniformly around the polyoxoanion, although the two cap ends of the Dawson-type polyoxoanion are not equivalent. All cations, except for Na (2), which is bonded only to one CH₃CN and five water molecules, are bonded to at least one oxygen atom of the polyoxoanion in addition to water, while Na (1) bridges two adjacent polyoxoanions and Na (6) and Na (7) each bridge three polyoxoanions. The packing diagram for Na₉P₂W₁₅Nb₃O₆₂ shows a Na⁺ "cloud" that surrounds each polyoxoanion with Na⁺...O-M (M=Nb, W) distances of 2.3–2.5 Å. *The multiple-bridging Na⁺ ions contribute to the solid-state ion-pairing interactions, which are formed between the Na⁺ ion and primarily the more basic Nb₃O₆ cap of the P₂W₁₅Nb₃O₆₂⁹⁻ polyoxoanion.* The solid-state ion-pairing interactions also persist even in nonaqueous solutions, which have caused the line-broadening and the additional smaller peaks of ³¹P resonance of the PO₄ moiety closer to the Nb₃O₆ site, as observed in the ³¹P NMR measured in DMSO-*d*₆ solution of [(*n*-C₄H₉)₄N]₅Na₃{[(cod)Ir](P₂W₁₅Nb₃O₆₂)}. This ion-pairing effect can be readily removed by adding three equivalents of the cryptand Kryptofix 2.2.2.^{1g,1h)}

The solid-state ³¹P NMR spectra observed here show that such solid-state ion-pairing interactions between the cation and the Nb₃O₆ site of the polyoxoanion commonly exist in other cation salts as well.

Conclusion

In conclusion, the water-soluble alkali metal salts of the Dawson-type heteropolyoxoanion, M₉P₂W₁₅Nb₃O₆₂ (M=Li, K, Cs), have been isolated, in 76, 63, and 47% yields and on a 1.9, 2.6, and 2.3-g scale, and have been unequivocally characterized, both in solution and in the solid state. The effects of the alkali-metal countercations on the P₂W₁₅Nb₃O₆₂⁹⁻ were observed in the solid state (as a cation-dependent thermal-stability), and also in the spectral changes of the ³¹P signal of the PO₄ unit closer to the Nb₃O₆ site in the Dawson structure. The order of the relative thermal-stability in the solid state was found to be: Cs salt **3** > K salt **1** >> Na salt **4** > Li salt **2**. In the solid-state ³¹P NMR spectra, the effect of the countercation was clearly observed particularly in the downfield signal. The solid-state ³¹P NMR spectral changes at elevated temperature were dependent upon both the degree of hydration at room temperature and the dehydration processes during heating. The fact that the downfield signal was markedly effected by the countercation was primarily interpreted in terms of solid-state ion-pairing interactions between the cation and the P₂W₁₅Nb₃O₆₂⁹⁻ polyoxoanion. The title complexes are also of interest as possible new type of solid-base catalysts; studies of such catalyses are planned.^{3e)}

The authors thank Professor R. G. Finke, Colorado State University, for his helpful suggestions concerning this work.

One of us (K.N.) also gratefully acknowledges financial support from Grant-in-Aid for Scientific Research (C) No. 06640735 of the Ministry of Education, Science and Culture.

References

- 1) a) K. Nomiya, M. Kaneko, N. C. Kasuga, R. G. Finke, and M. Pohl, *Inorg. Chem.*, **33**, 1469 (1994); b) D. J. Edlund, R. J. Saxton, D. K. Lyon, and R. G. Finke, *Organometallics*, **7**, 1692 (1988); c) K. Nomiya, M. Pohl, N. Mizuno, D. K. Lyon, and R. G. Finke, *Inorg. Synth.*, **31**, 186 (1997); d) M. Pohl, Y. Lin, T. J. R. Weakley, K. Nomiya, M. Kaneko, H. Weiner, and R. G. Finke, *Inorg. Chem.*, **34**, 767 (1995); e) K. Nomiya, C. Nozaki, M. Kaneko, R. G. Finke, and M. Pohl, *J. Organomet. Chem.*, **505**, 23 (1995); f) R. G. Finke, D. K. Lyon, K. Nomiya, and T. J. R. Weakley, *Acta Crystallogr., Sect. C*, **C46**, 1592 (1990); g) R. G. Finke, D. K. Lyon, K. Nomiya, S. Sur, and N. Mizuno, *Inorg. Chem.*, **29**, 1784 (1990); h) M. Pohl, D. K. Lyon, N. Mizuno, K. Nomiya, and R. G. Finke, *Inorg. Chem.*, **34**, 1413 (1995); i) The more improved synthesis of the monomer [(*n*-C₄H₉)₄N]₉P₂W₁₅Nb₃O₆₂, without the dimer preparation, has been recently found. H. Weiner, J. D. Aiken, and R. G. Finke, *Inorg. Chem.*, **35**, 7905 (1996); j) K. Nomiya, K. Nomura, and T. Taguchi, "72th Annual Meeting of the Chemical Society of Japan," Tokyo, 1997, Abstr., No. IPA069.
- 2) For example: A. Corma, *Chem. Rev.*, **95**, 559 (1995).
- 3) a) D. K. Lyon and R. G. Finke, *Inorg. Chem.*, **29**, 1787 (1990); b) N. Mizuno, D. K. Lyon, and R. G. Finke, *J. Catal.*, **128**, 84 (1991); c) Y. Lin and R. G. Finke, *J. Am. Chem. Soc.*, **116**, 8335 (1994); d) M. Pohl, Dissertation, University of Oregon, 1994; e) M. Barteau, K. Nomiya, and R. G. Finke, Experiments in progress.
- 4) K. Nomiya, C. Nozaki, A. Kano, T. Taguchi, and K. Ohsawa, *J. Organomet. Chem.*, (1997), in press.
- 5) P. A. Van Der Meulen and H. L. Van Mater, *Inorg. Synth.*, **1**, 24 (1939).
- 6) Solid CsBF₄ was isolated as colorless, needle crystals by a stoichiometric reaction of 9.6 mL (46 mmol) of 30% aqueous HBF₄ solution with 6.9 g (46 mmol) of CsOH in 20 mL water, followed by recrystallization from 60 mL water. Yield: 3.3 g (44%). The FT-IR spectrum measured as KBr disk: 1654s, 1302m, 1082s, 1027s, 525m cm⁻¹.
- 7) In more precise TG/DTA measurements, done with a temperature ramp of 1 °C min⁻¹ for Keggin-type heteropolytungstates containing only solvated waters, weight loss of 9.40% (calcd for 16 hydrated water, 9.45%) has been observed below 300 °C with an endothermic point at 91 °C for analytically pure Na₇SiW₉Nb₃O₄₀·16H₂O.⁴⁾
- 8) C. Rocchioccioli-Deltcheff and R. Thouvenot, *Spectrosc. Lett.*, **12**, 127 (1979).
- 9) a) Y. Kanda, K. Y. Lee, S. Nakata, S. Asaoka, and M. Misono, *Chem. Lett.*, **1988**, 139; b) S. Hayashi and K. Hayamizu, *Bull. Chem. Soc. Jpn.*, **62**, 3061 (1989); c) J. B. Black, N. J. Clayden, L. Griffiths, and J. D. Scott, *J. Chem. Soc., Dalton Trans.*, **1984**, 2765; d) R. Contant, C. Rocchioccioli-Deltcheff, M. Fournier, and R. Thouvenot, *Colloids Surfaces A*, **72**, 301 (1993); e) W. E. Farneth, R. H. Staley, P. J. Domaille, and R. D. Farlee, *J. Am. Chem. Soc.*, **109**, 4018 (1987).